Applied Catalysis A: General 435–436 (2012) 10–18

Contents lists available at SciVerse ScienceDirect

Applied Catalysis A: General

journal homepage: www.elsevier.com/locate/apcata

Influence of Pt addition to Ni catalysts on the catalytic performance for long term dry reforming of methane

S.R. de Miguel [a], I.M.J. Vilella [a,*], S.P. Maina [a], D. San José-Alonso [b], M.C. Román-Martínez [b], M.J. Illán-Gómez [b]

[a] Instituto de Investigaciones en Catálisis y Petroquímica (INCAPE), Facultad de Ingeniería Química, Universidad Nacional del Litoral, CONICET, Santiago del Estero 2654, 3000 Santa Fe, Argentina
[b] Departamento de Química Inorgánica, Universidad de Alicante, Ap. 99, E-03080 Alicante, Spain

ARTICLE INFO

Article history:
Received 15 March 2012
Received in revised form 16 May 2012
Accepted 20 May 2012
Available online 27 May 2012

Keywords:
Methane dry reforming
PtNi catalysts
Alumina-based catalysts
Catalyst deactivation

ABSTRACT

The influence of Pt addition (in very low concentrations) to a Ni/(10%)/Al_2O_3 catalyst in its catalytic performance during long-term experiments of dry reforming of methane was studied.

The monometallic Pt(0.5%)/Al_2O_3 catalyst displayed a pronounced deactivation during 6500 min reaction time, mainly due to a significant sintering of the metallic phase, whereas the monometallic Ni(10%)/Al_2O_3 catalyst showed a high and stable activity along the reaction time.

Compared with the Ni(10%)/Al_2O_3 catalyst, the bimetallic Ni(10%)Pt(0.5%)/Al_2O_3 sample showed a higher, and stable catalytic activity during the 6500 min reaction time and a markedly lower carbon deposition. TEM images reveal much less carbon formation and filament grow and this leads to expect a higher stability in long term processes. Characterization techniques indicate that nickel and platinum are in close contact during the simultaneous reduction of the two oxide precursors and that geometric effects (dilution and blocking) are mainly responsible for the excellent catalytic behaviour of the bimetallic NiPt catalyst.

1. Introduction

Processes like steam reforming and partial oxidation of methane are commonly used to transform natural gas into synthesis gas or more valuable products. Due to the extended use of synthesis gas as feedstock for several chemical processes, i.e. fuel cells, methanol synthesis and Fischer–Tropsch reaction [1–7], there has been an increasing interest in the production of synthesis gas from natural gas by the CO_2-reforming of methane, also called dry reforming of methane (DRM). Additionally, DRM provides low H_2/CO ratios required for hydroformylation and carbonylation reactions.

In spite of the initial difficulties, the study of the methane reforming with CO_2 has been progressively increased. A very important driving force to develop new technologies and catalysts is derived from the potential application of this process for the preservation of the environment, since CO_2 plays an important role in the greenhouse effect. Furthermore, a comparative study about the production of acetic acid using three processes – that is, the steam reforming, the partial oxidation and the CH_4 reforming with CO_2 – it was concluded that the operative cost of the methane reforming with CO_2 is lower than those of the other two processes [8]. Hence, this process seems to be a promising route from an economic point of view and it also appears an adequate tool for the environmental protection.

The commonly used catalysts for the DRM reaction are Ni-based ones. Unfortunately, under reforming conditions, carbon deposits could block the catalyst pores and encapsulate the active sites, which would lead to the catalyst deactivation [3,9,10]. However, carbon formation can be reduced or suppressed by using adequate promoters and supports. With respect to promoters, Juan-Juan et al. [11] studied the effect of the potassium content in the structure and properties of the Ni active phase and in the activity and selectivity of NiK/Al_2O_3 catalysts for DRM. Besides, it is well known that noble metals inhibit coke formation. Moreover, it has been reported that the addition of noble metals to Ni catalysts can promote the reducibility of Ni, and stabilize its degree of reduction during the catalytic process [12–14]. Chen et al. [12] found that the noble metal addition to Ni improves the catalyst stability and reducibility. Tomishige et al. [14] observed that the catalytic activity for the autothermal reforming of methane was increased when small amounts of Pt were added to Ni/Al_2O_3 catalysts. Pawelec et al. [3] reported, for bimetallic PtNi catalysts supported on ZSM-5, an improvement of the catalytic activity and stability for DRM, which was attributed to an increase of the nickel dispersion caused by the

* Corresponding author. Tel.: +54 342 4555279; fax: +54 342 4555279.
E-mail address: jvilella@fiq.unl.edu.ar (I.M.J. Vilella).

0926-860X/$ – see front matter © 2012 Elsevier B.V. All rights reserved.
http://dx.doi.org/10.1016/j.apcata.2012.05.030

intimate contact between nickel and platinum. Besides, Rh and Pd addition to Ni-supported catalysts has also been studied [15–17]. In this way, Ocsachoque et al. [15] using NiRh catalysts supported on alumina modified by CeO_2 found good stability and activity and high resistance to carbon formation whereas Wu et al. [16] worked with Rh–Ni supported on boron nitride and alumina and found promising results with the first support in what methane conversion, hydrogen yield and coke reduction it concerns. On the other hand, Steinhauer et al. [17] studied the Ni–Pd performance over different supports and conclude that the system supported on Al_2O_3 and TiO_2 did not give good catalytic activity in the DRM.

The aim of the present work is to develop new and effective supported Ni catalysts modified with a small amount of noble metal in order to obtain relatively cheap supported bimetallic catalysts with an improved catalytic behaviour (activity and stability) for the DRM, during long term reactions. Even though there are works dealing with this catalytic system, a research over long-term reaction (of about 100 h reaction time) was not found.

2. Experimental

An alumina-supported nickel catalyst (Ni(10%)/Al_2O_3) was prepared by excess-solution impregnation using a pelletized γ-Al_2O_3 support (supplied by Across, S_{BET} = 90 $m^2\,g^{-1}$) and an aqueous solution of $Ni(NO_3)_2{\cdot}6H_2O$ of the appropriate concentration to obtain a 10 wt% nickel content. After impregnation, the samples were dried overnight at 100 °C. Bimetallic catalysts with 0.2 and 0.5 wt% Pt (samples Pt(0.2%)Ni(10%)/Al_2O_3 and Pt(0.5%)Ni(10%)/Al_2O_3) were prepared by impregnation of the Ni(10%)/Al_2O_3 sample (previously ground to a particle size between 35 and 80 mesh) with a solution of chloroplatinic acid at room temperature. The impregnation volume/support weight ratio was 1.4 ml g^{-1}. After impregnation, the catalysts were dried overnight at 100 °C. Besides, monometallic Pt(0.2%)/Al_2O_3 and Pt(0.5%)/Al_2O_3 samples were prepared by impregnation of the γ-Al_2O_3 support (35–80 mesh) with an aqueous solution of chloroplatinic acid and following a procedure similar to that indicated above.

The acidic properties of the alumina support were determined by the isopropanol (IPA) dehydration reaction at 230 °C and atmospheric pressure in a flow reactor, using a H_2/IPA molar ratio equal to 18 and a space rate of 32 h^{-1}.

The basic character of the support was determined by CO_2 adsorption and desorption experiments. The CO_2 adsorption was carried out at room temperature using a flow of CO_2 (5%)/N_2 (50 ml min^{-1}), and the desorption was studied by Temperature Programmed Desorption (TPD) conducted from 25 °C up to 500 °C at 5 °C min^{-1} using a thermal conductivity detector to measure the response.

The reducibility of the catalysts was studied by Temperature Programmed Reduction (TPR) using a reducing mixture composed by H_2 (5%, v/v)/N_2 with a flow rate of 10 ml min^{-1} and a heating rate of 6 °C min^{-1} from room temperature up to 750 °C.

The metallic dispersion was determined by H_2 chemisorption and the state of the metallic phase was studied using the cyclohexane (CH) dehydrogenation as test reaction. The H_2 chemisorption measurements were carried out at 25 °C in a volumetric equipment. The catalyst was previously reduced with H_2 at 750 °C for 3 h, and then it was outgassed under high vacuum (10^{-4} Torr) at the same temperature for 1 h. Once the sample was cooled down to room temperature, the chemisorption test began. The test reaction (cyclohexane (CH) dehydrogenation) at 300 °C was performed in a differential flow reactor at atmospheric pressure, by using a H_2/CH molar ratio of 29 and a CH flow rate of 6 ml h^{-1}. The activation energy of the different catalysts for CH dehydrogenation was obtained by measuring the initial reaction rate at 315, 300 and 285 °C. The reaction products were analysed by gas chromatography (Chromatograph Varian Star 3400, Chromosorb packed column and TCD as detector).

The DRM reaction was carried out in a flow equipment at 700 °C during 360 min. The samples (0.17 g) were first reduced under flowing H_2 at 750 °C for 3 h. After reduction, He was passed through the catalyst bed for 15 min, and finally the CH_4/CO_2 mixture (CH_4/CO_2 molar ratio = 1) was fed to the reactor with a flow rate of 20 ml min^{-1}. In order to avoid diffusion effects, catalyst particle sizes were very small (between 0.18 and 0.42 mm). The reaction products were analysed by gas chromatography (using a Supelco Carboxen 1006 PLOT (30 m × 0.53 mm) column and a TCD detector). In order to study the catalyst stability, additional experiments at 750 °C were performed during longer reaction times (6500 min).

XPS analysis was carried out in a Multitechnic UniSpecs Photoemission Electron Spectrometer equipped with an X-ray source Mg/Al and a hemispherical analyser PHOIBOS 150 in the fixed analyser transmission mode (FAT). The spectrometer operates with an energy power of 100 eV and the spectra were obtained with pass energy of 30 eV and a Mg anode operated at 100 W. Samples were previously reduced under H_2 at 750 °C for 3 h in a flow reactor and then, they were introduced in the equipment and reduced "in situ" with H_2 at 400 °C for 1 h. The binding energies (BE) were referred to the C1s peak at 284 eV. Peak areas and BE values were estimated by fitting the curves with combination of Lorentzian–Gaussian curves of variable proportion using the CasaXPS Peak-fit software version 1.2.

The amount of carbon accumulated was determined by Temperature Programmed Oxidation (TPO) experiments: the used catalyst was submitted to a heat treatment in a O_2:He (16:84) flow (110 ml min^{-1}) at 20 °C min^{-1} up to 900 °C. The experiments were performed in a TA SDT-680 thermobalance coupled to a mass spectrometer (Balzers Quadstar). Thus, the amount of carbon burned out was determined by the weight loss and by the amount of CO_2 and CO evolved, calculated by analysis of signals m/z = 44 and 28, respectively. The experimental error in the determination of deposited carbon is about 3%.

Transmission electron microscopy (TEM) analysis was performed using a JEOL JEM-2010 microscope working in the acceleration range of 100–200 kV. The line resolution is 0.14 nm and the point resolution is 0.25 nm.

3. Results

3.1. Acidity and basicity of the support

The isopropanol (IPA) dehydration capacity of the γ-Al_2O_3 Across is negligible at 230 °C (IPA conversion < 0.2%) and much lower than that corresponding to an acidic alumina like CK-300 at the same temperature (IPA conversion = 8%), thus indicating the low acidity characteristics of the γ-Al_2O_3.

The CO_2-TPD profile of the γ-Al_2O_3 (not showed here) showed a practically negligible CO_2 desorption zone at very low temperatures (100–150 °C), which indicates the low basicity of the support.

3.2. Catalytic activity and stability

The catalytic properties of the two monometallic Pt catalysts (0.2 and 0.5 wt% Pt) and the monometallic Ni(10 wt%) catalyst were evaluated in the methane reforming with CO_2 at 700 °C. The results of CO_2 and CH_4 conversion at different times are listed in Table 1. The comparison between both Pt catalysts shows that the sample with the higher metal content is not only more active but also more stable, mainly during the first 3 h reaction time. This fact is observed for both CH_4 and CO_2 conversions. On the other hand,

Table 1
Dry reforming of methane at 700 °C. CH_4 and CO_2 conversions for monometallic catalysts.

Catalyst	X_{CH_4} (%)				X_{CO_2} (%)			
	0 h	1 h	3 h	6 h	0 h	1 h	3 h	6 h
$Pt(0.2\%)/Al_2O_3$	42	23	12	8	50	28	15	10
$Pt(0.5\%)/Al_2O_3$	51	41	31	13	58	47	35	16
$Ni(10\%)/Al_2O_3$	70	71	70	70	77	78	76	77

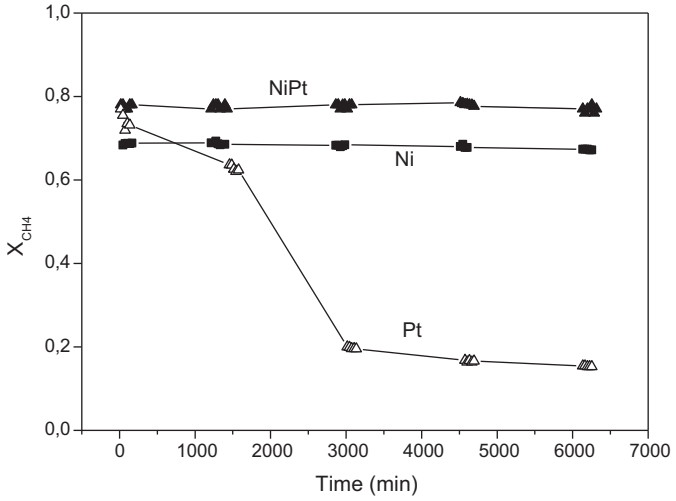

Fig. 1. CH_4 conversion at 750 °C during 6500 min reaction time for $Pt(0.5\%)/Al_2O_3$, $Ni(10\%)/Al_2O_3$ and $Pt(0.5\%)Ni(10\%)/Al_2O_3$ catalysts.

$Ni(10\%)/Al_2O_3$ catalyst shows a very good activity and stability during the whole reaction time.

In order to compare the catalytic behaviour of a PtNi catalyst with the corresponding monometallic ones and taking into account the above-mentioned results, a sample with 10 wt% Ni and 0.5 wt% Pt was selected for the study. Thus, $Pt(0.5\%)/Al_2O_3$, $Ni(10\%)/Al_2O_3$ and $Pt(0.5\%)Ni(10\%)/Al_2O_3$ catalysts were submitted to very long DRM experiment (6500 min) at 750 °C. Results of CH_4 conversion, CO_2 conversion and the obtained H_2/CO molar ratio as a function of the reaction time are shown in Figs. 1–3, respectively.

The $Pt(0.5\%)/Al_2O_3$ catalyst shows a slight decay in both CH_4 and CO_2 conversions (Figs. 1 and 2) during the first 24 h of reaction, then a pronounced deactivation during the following 24 h is observed and finally, the conversion remains practically constant, this being close to 20%. The amount of coke (determined by TPO experiments) after the 6500 min reaction time was very low (0.46 wt%), thus indicating that the carbon deposition was probably not the main factor responsible of the catalyst deactivation.

As shown in Figs. 1 and 2 the activity of the monometallic $Ni(10\%)/Al_2O_3$ catalyst is constant along the 6500 min reaction time, being both CH_4 (≅67%) and CO_2 conversions (≅89%) stable. The activity of the bimetallic $Pt(0.5\%)Ni(10\%)/Al_2O_3$ catalyst also remains constant along the 6500 min reaction time, but both CH_4 (≅78%) and CO_2 conversion (≅95%) are higher than those corresponding to $Ni(10\%)/Al_2O_3$ catalyst. Regarding the amount of deposited carbon determined by TPO experiments, it is much larger for the monometallic $Ni(10\%)/Al_2O_3$ catalyst (22 wt%) than for the bimetallic catalyst $Ni(10\%)Pt(0.5\%)/Al_2O_3$ (7 wt%).

With respect to the H_2/CO molar ratio, Fig. 3 shows that the monometallic Pt catalyst gives a high molar ratio (0.70) during the first hour of the reaction time, but it decreases up to 0.40 after 48 h reaction time. The molar ratio produced by the bimetallic NiPt catalyst (0.63) is slightly higher than that found for the Ni sample (0.59) and these values remain constant during the reaction time. These data indicate that H_2/CO molar ratio values are lower than that expected one from the stoichiometry of the DRM reaction (1). This implies a certain extent of the reverse water gas-shift reaction (RWGS), since this reaction consumes part of the produced H_2 to react with CO_2, yielding CO and water.

It is worth noticing that the $Pt(0.5\%)Ni(10\%)/Al_2O_3$ catalyst shows a very good catalytic performance (activity, selectivity and H_2/CO_2 molar ratio), which is better than that of the $Ni(10\%)/Al_2O_3$ catalyst and of the $Pt(0.5\%)/Al_2O_3$ catalyst which displays the lowest CH_4 and CO_2 conversions, and also the lowest H_2/CO molar ratio after 2000 min reaction time.

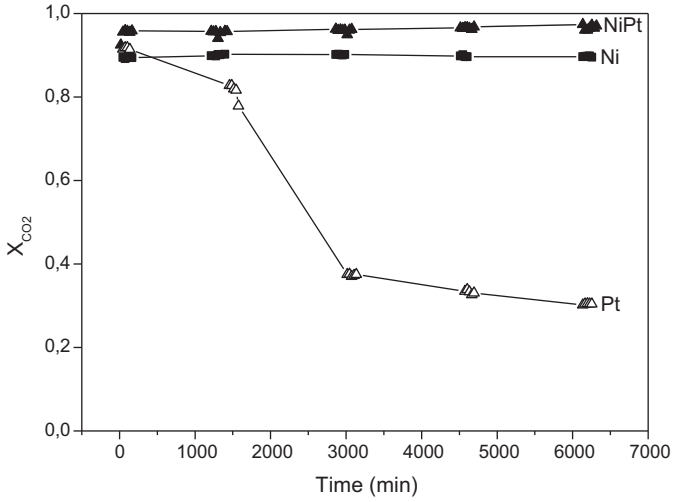

Fig. 2. CO_2 conversion at 750 °C during 6500 min reaction time for $Pt(0.5\%)/Al_2O_3$, $Ni(10\%)/Al_2O_3$ and $Pt(0.5\%)Ni(10\%)/Al_2O_3$ catalysts.

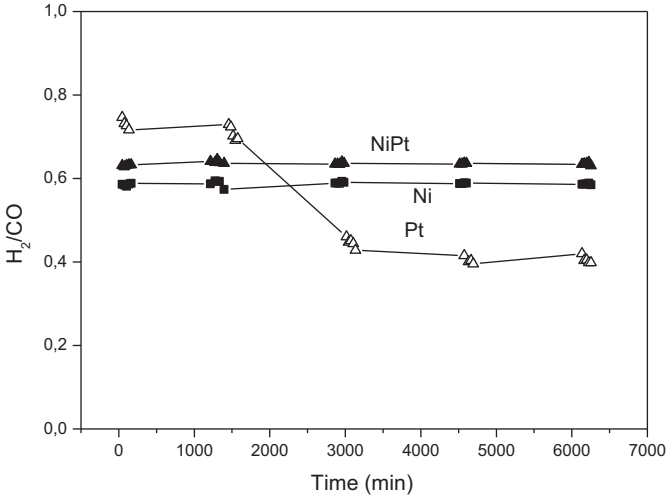

Fig. 3. H_2/CO molar ratio obtained for $Pt(0.5\%)/Al_2O_3$, $Ni(10\%)/Al_2O_3$ and $Pt(0.5\%)Ni(10\%)/Al_2O_3$ catalysts (750 °C, 6500 min reaction time).

Table 2
Results of H_2 chemisorption and a cyclohexane dehydrogenation reaction for the different catalysts.

Catalyst	H_T (μmol H_2 g cat^{-1})	D (%)	R_{CH} (mol h^{-1} g metal^{-1})	$E_{Act.}$ (kcal mol^{-1})
Pt(0.2%)/Al_2O_3	1.7	33	135	18.8
Pt(0.5%)/Al_2O_3	3.5	27	81	16.4
Ni(10%)/Al_2O_3	44	5	<2	–
Pt(0.2%)Ni(10%)/Al_2O_3	42	–	76	14.8
Pt(0.5%)Ni(10%)/Al_2O_3	28	–	68	16.0

3.3. Catalyst characterization

3.3.1. H_2 chemisorption and test reaction

Table 2 shows the results corresponding to H_2 chemisorption measurements (and the calculated dispersion values for the monometallic catalysts). The Pt dispersion in sample Pt(0.2%)/Al_2O_3 is slightly higher than in Pt(0.5%)/Al_2O_3 catalyst, as it can be inferred from the H_2 chemisorption values. On the other hand, the monometallic Ni catalyst shows a considerable lower metal dispersion. Data obtained for the bimetallic catalysts show that the Pt addition to Ni(10%) reduces the chemisorption of H_2 by Ni, this effect being more pronounced in the case of Pt(0.5%)/Al_2O_3 catalyst. The lower H_2 chemisorption in the bimetallic catalysts is likely due to geometric effects, that is Pt would be deposited over Ni particles reducing the accessible sites in this way.

Table 2 also includes the results for the cyclohexane (CH) dehydrogenation, a structure-insensitive reaction used as a test reaction of the metallic phase. In the case of the monometallic Pt catalysts, the increase of the metal content from 0.2 to 0.5 wt% produces a decrease in the activity for CH dehydrogenation, which is in agreement with the dispersion results. Ni(10%)/Al_2O_3 catalyst presents a practically negligible activity for this reaction at 300 °C, and the bimetallic NiPt catalysts display an activity lower than that corresponding to Pt(0.5%)/Al_2O_3 catalyst, thus indicating a lower amount of active sites. This supports the idea of a certain blocking effect of Ni on Pt. Considering, as well, the previously commented H_2 chemisorption data, it can be considered that Pt and Ni are in close contact and this produces a reduction of the active sites in both metals compared to the monometallic catalysts.

Taking into account that CH dehydrogenation is a structure-insensitive reaction [18], the similar values of the activation energy for both bimetallic catalysts with respect to the corresponding monometallic Pt/Al_2O_3 one would indicate that the electronic modifications of the active phase are not significant. However, as mentioned above and deduced from CH dehydrogenation activity

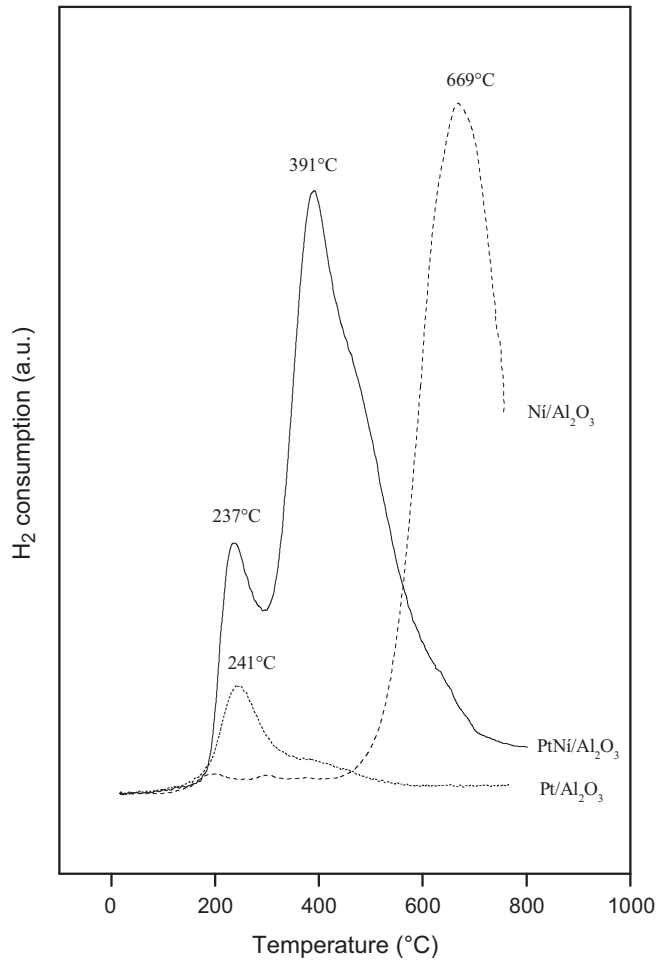

Fig. 4. TPR profiles of Pt(0.5%)/Al_2O_3, Ni(10%)/Al_2O_3 and Pt(0.5%)Ni(10%)/Al_2O_3 catalysts.

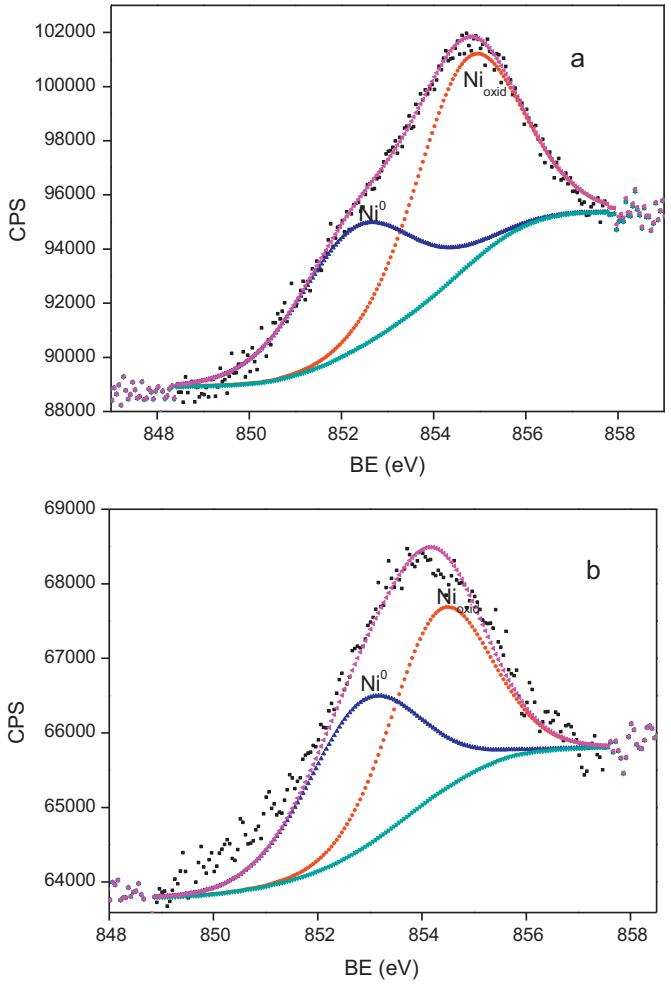

Fig. 5. Ni2p XPS signals for Ni(10%)/Al_2O_3 catalyst before (a) and after (b) long reaction.

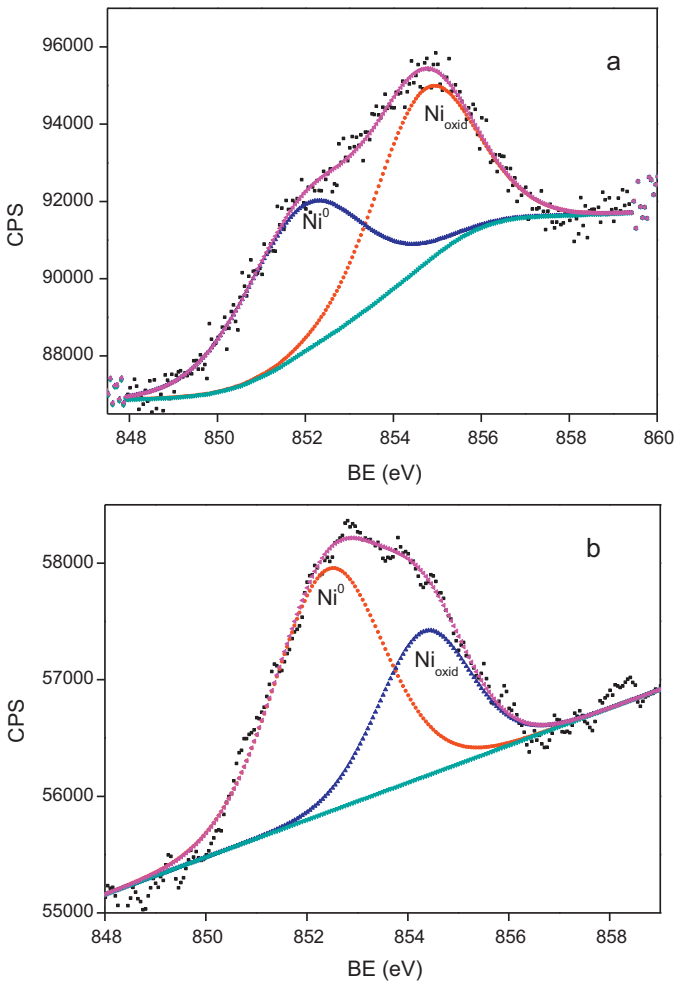

Fig. 6. Ni2p XPS signals for Pt(0.5%)Ni(10%)/Al_2O_3 catalyst before (a) and after long reaction (b).

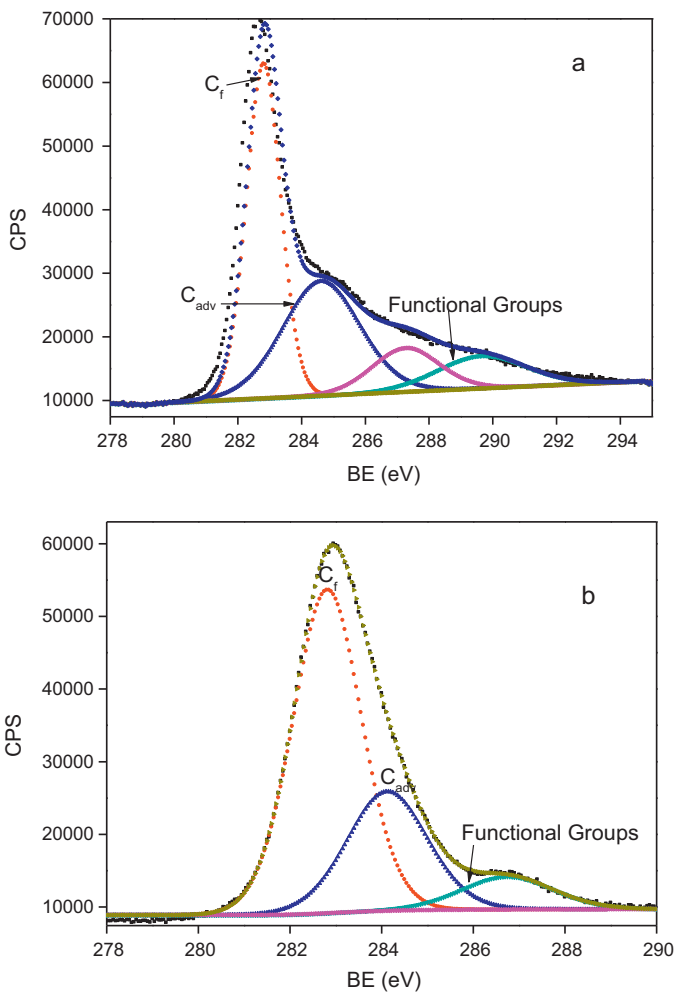

Fig. 7. C1s XPS signals for Ni (a) and NiPt (b) samples after long reaction.

and chemisorption measurements, geometric effects (dilution and blocking) are relevant for this bimetallic catalyst.

The used Pt(0.5%)/Al_2O_3 catalyst (after 6500 min reaction time in dry reforming of methane) was also evaluated in the CH dehydrogenation reaction. It was previously submitted to a smooth oxidation in air (100 ml min^{-1}) at 400 °C for 2 h to eliminate the low amount of coke formed during reaction. The activity for CH dehydrogenation decreased from 81 to 15 mol h^{-1} gPt^{-1}; hence the deactivation of the Pt(0.5%)/Al_2O_3 sample during the dry reforming of methane can be attributed to a sintering process taking place during the long-time reaction, which would produce a pronounced increase of the platinum particles size.

3.3.2. Temperature programmed reduction (TPR)

Fig. 4 shows the TPR profiles obtained for Pt(0.5%)/Al_2O_3, Ni(10%)/Al_2O_3 and Pt (0.5%)Ni(10%)/Al_2O_3 samples. The TPR profile of the monometallic platinum catalyst shows a main reduction peak at 241 °C and a very small shoulder at 400 °C, which can be explained by the existence of different oxychlorinated Pt species originated after the impregnation of the support with chloroplatinic acid and the subsequent thermal treatments (drying and calcination steps) [19]. The profile corresponding to the monometallic Ni catalyst shows a very pronounced and wide peak with a maximum at 669 °C, which corresponds to the expected reduction of NiO in intimate contact with alumina supports [11,20]. The TPR profile obtained for the bimetallic NiPt catalyst shows two peaks: one at 237 °C corresponding to the reduction of Pt species, and another one at 391 °C attributed to the reduction of NiO in intimate contact with alumina. The reduction of these species occurs at such a lower temperature due to the presence of Pt, because Pt particles already formed could activate hydrogen, thus favouring the reduction of nickel oxide, The occurrence of this effect during the simultaneous reduction of the two oxide precursors is a consequence of the close contact of nickel and platinum previously suggested (revealed by H_2 chemisorption and test reaction results). The close contact between metal precursors would result in a mixture of metal particles that produces the mentioned geometric effects and not in the formation of Pt–Ni clusters as postulated by Pawelec et al. [3]

3.3.3. XPS results

XPS spectra of Ni2$p_{3/2}$ for Ni and NiPt catalysts before and after the long-time DRM experiments are presented in Figs. 5 and 6, respectively. Besides, Table 3 summarizes the binding energies, the percentages of each Ni species (between parentheses) and the surface atomic ratios (calculated from the peak intensities of the peak normalized by atomic sensitivity factors [21]) of the Al2p and Ni2$p_{3/2}$ core electrons for the Ni and NiPt catalysts before and after reaction.

It can be seen that in fresh Ni(10%)/Al_2O_3 catalyst (before reaction), two Ni species were detected: one at 852.3 eV, due to metallic Ni, and the another one at 854.7 eV corresponding to NiO [21]. The used monometallic Ni(10%)/Al_2O_3 catalyst (after reaction) displays

Table 3
XPS results for the different catalysts (before and after reaction). Binding energies (BE), percentages of Ni surface species (between parentheses) and surface atomic ratios.

Catalyst	Ni2p		C1s	
Ni/Al_2O_3 before reaction	Ni^0 NiO Ni/Al = 65.8%	852.3 eV (40%) 854.7 eV (60%)		
Ni/Al_2O_3 after reaction	Ni^0 NiO Ni/Al = 46.5%	852.8 eV (53%) 854.4 eV (47%)	Filamentous carbon Graphitic carbon C—O Groups	282.6 eV 284.1 eV 288.1 eV
$PtNi/Al_2O_3$ before reaction	Ni^0 NiO Ni/Al = 43.3%	851.9 eV (50%) 854.7 eV (50%)		
Pt Ni/Al_2O_3 after reaction	Ni^0 NiO Ni/Al = 32.3%	852.4 eV (67%) 854.3 eV (33%)	Filamentous carbon Graphitic carbon C—O Groups $Surf.C_{PtNi}/Surf.C_{Ni} = 0.73$	282.8 eV 284.1 eV 286.7 eV

signals corresponding both to metallic (852.8 eV) and oxidized (854.4 eV) Ni species, though the relative proportion of Ni^0 in this sample is higher (53%) than in the fresh reduced monometallic sample (40%) (Fig. 5a and b). For the $Pt(0.5\%)Ni(10\%)/Al_2O_3$ catalyst (Fig. 6a and b before and after reaction, respectively) two different signals associated with Ni^0 (851.9–852.4 eV) and NiO (854.3–854.7 eV) were registered. Before reaction, the percentage of metallic nickel in the $Pt(0.5\%)Ni(10\%)/Al_2O_3$ catalyst (50%) is higher than in the $Ni(10\%)/Al_2O_3$ catalyst (40%) (Table 3). This indicates that the addition of Pt favours the reducibility of Ni oxide to metallic species. This is in agreement with the easier reduction of NiO species in the bimetallic catalyst deduced from TPR results (Fig. 4). Besides, it must be pointed out that during the long-time reforming reaction the Ni^0 content clearly increases: from 40 to 53% in the Ni/Al_2O_3 catalyst, and from 50 to 67% in the $Pt(0.5\%)Ni(10\%)/Al_2O_3$ catalyst (Table 3). Both the presence of reaction products with a strong reducing effect, as H_2 and CO, and the high reaction temperature, would be responsible for the

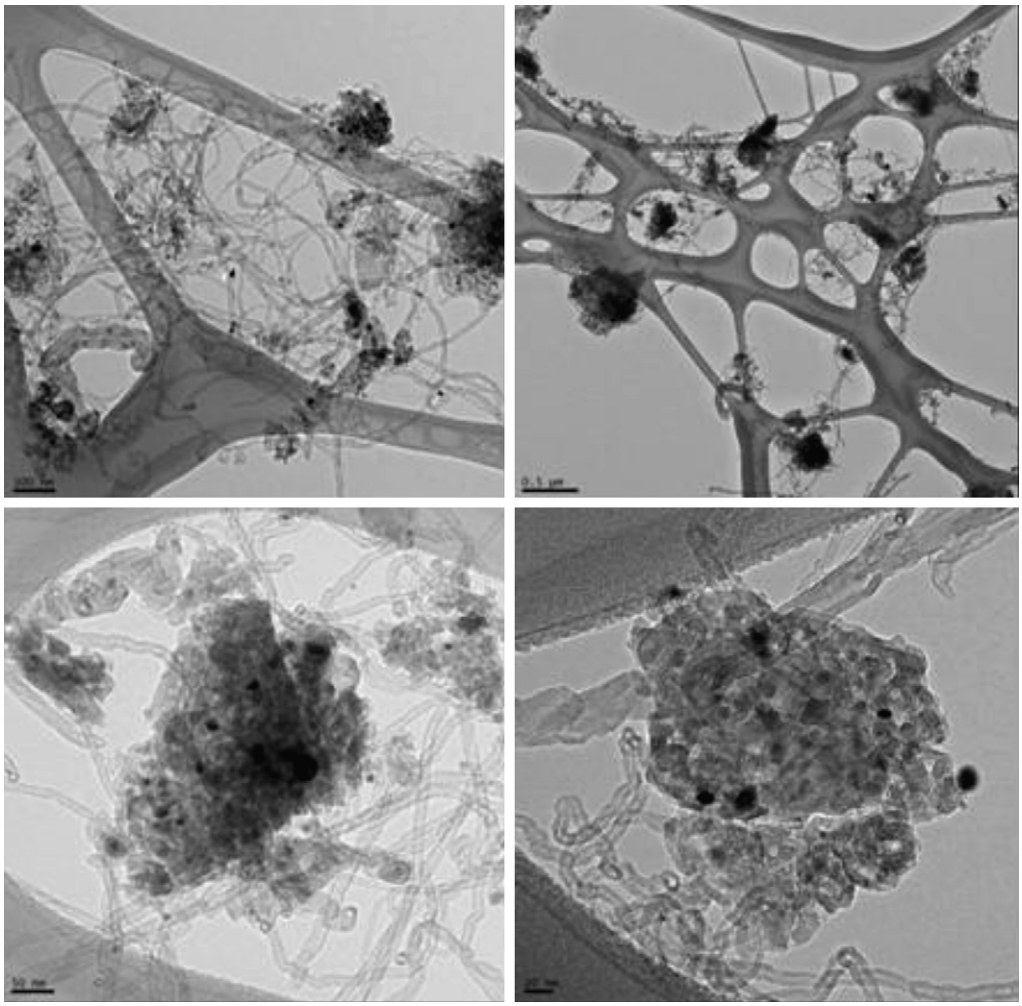

Fig. 8. TEM microphotographies of used $Ni(10\%)/Al_2O_3$ catalyst after DRM reaction at 750 °C during 6500 min.

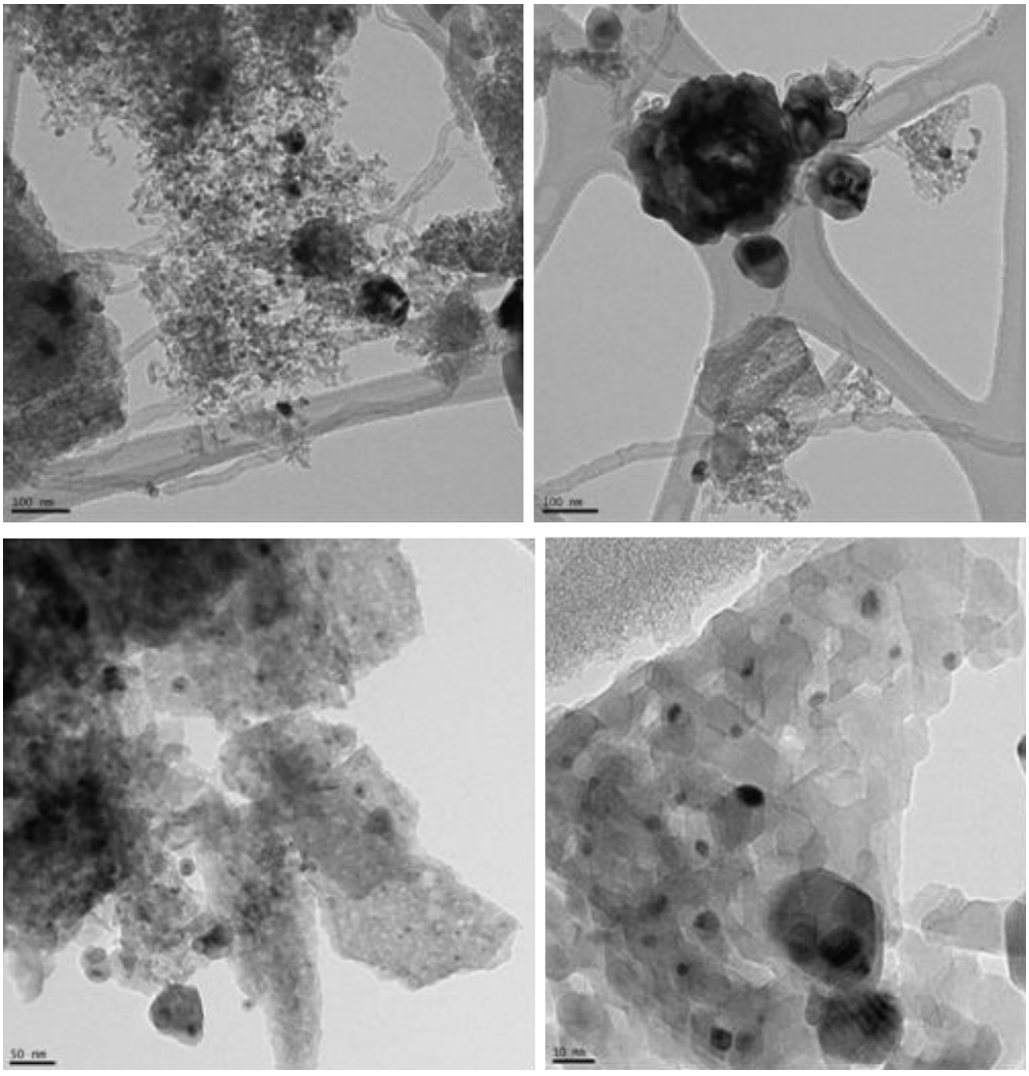

Fig. 9. TEM microphotographies of used Pt(0.5%)Ni(10%)/Al_2O_3 catalyst after DRM reaction at 750 °C during 6500 min.

higher reduction of Ni species during reaction. The BE of Pt $4d_{5/2}$ at 314.0 eV observed for the reduced PtNi catalyst indicates the presence of only Pt^0.

It can be also observed in Table 3 that the Ni/Al surface ratios (both for Ni and PtNi catalysts) decreased after reaction, but this decrease is less pronounced for the PtNi catalyst than for the monometallic Ni catalyst. This indicates that, as observed by García Diéguez et al. [22], Ni species on the catalyst surface can be stabilized during reaction by the close presence of Pt.

In order to determine the properties of the carbon deposited on the surface of the used catalysts, XPS spectra of C1s core electrons for used Ni(10%)/Al_2O_3 and Pt(0.5%)Ni(10%)/Al_2O_3 catalysts were also obtained. The obtained profiles are displayed in Fig. 7 where it is observed that similar types of carbon are deposited on the surface of both catalysts during the DRM reaction. Deconvolution of the C1s signal for both samples reveals the presence of a dominant peak at 282.6–282.8 eV, another one at 284.1 eV, characteristic of graphitic carbon, and a third and small one at 286.7–288.1 eV, that can be related to C—O contributions. The presence of these three carbon structures detected by XPS was similar to those determined by Pawelec et al. [3], but García-Diéguez et al. [22] found, besides the mentioned three signals, two important peaks between 278 and 280 eV, which were attributed by the authors to carbon nanofibers and carbon nanotubes. The C—O contributions were probably caused by the interaction of the CO_2 reagent with the alumina surface. The main peak of the C1s spectra corresponds to filamentous carbon species (C_f). It was also detected a signal of the so-called adventitious carbon (C_{adv}) whose nature does not appear to be graphitic and that it is generally comprised of a variety of hydrocarbon species with small amount of double and single bond oxygen functionalities [23].

The surface carbon (determined from XPS measurements and also shown in Table 3) in the PtNi catalyst is lower than in the monometallic Ni catalyst (about 27% lower), thus indicating that the addition of Pt to Ni produces a partial inhibition of the surface carbon deposition during the reaction, which is a positive effect which favours the stability of the catalysts.

3.3.4. TEM results

TEM images shown in Figs. 8–10 correspond to the Ni(10%)/Al_2O_3, Pt(0.5%)Ni(10%)/Al_2O_3 and Pt(0.5%)/Al_2O_3 catalysts, respectively, which were used for the dry reforming of methane at 750 °C during 6500 min.

The TEM images of the used monometallic Ni catalyst show a large amount of carbon formation and filament growth (Fig. 8), while in the case of the used PtNi catalyst (Fig. 9) the observed amount of carbon and the filament growth are noticeably lower. This is in agreement with the amount of deposited carbon

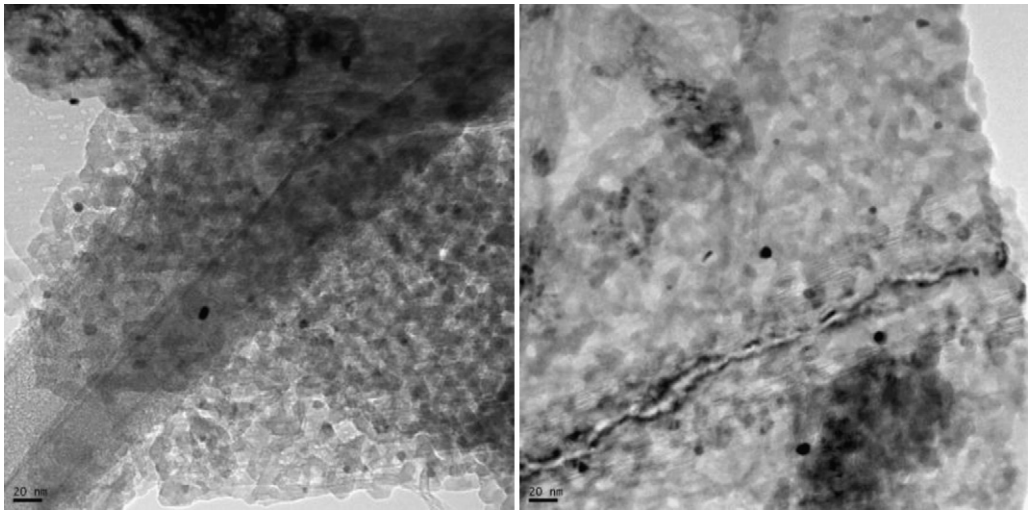

Fig. 10. TEM microphotographies of used Pt(0.5%)/Al_2O_3 catalyst after DRM reaction at 750 °C during 6500 min.

determined by TPO measurements: 7 wt% in the bimetallic PtNi catalysts and 22 wt% in the monometallic Ni one.

For the used Pt(0.5%)/Al_2O_3 catalyst, the presence of carbon was not observed by TEM (Fig. 10), in agreement with the very low amount of coke measured by TPO (only 0.46 wt%). For this used catalyst, Pt particles with sizes between 4 and 8 nm can be observed in TEM images. It must be mentioned that the fresh reduced Pt(0.5%)/Al_2O_3 catalyst was also examined by TEM and it was impossible to detect Pt particles, what can be interpreted as a very high Pt dispersion. These results confirm that the Pt particle size in the monometallic Pt catalyst noticeably increases during the long-time reaction carried out at 750 °C.

4. Discussion

The fresh monometallic Pt(0.5%)/Al_2O_3 catalyst shows a highly dispersed metallic phase and hence a good initial catalytic activity for the DRM reaction at 750 °C. However, after a few hours the catalyst begins to deactivate and the conversion decreases from more than 70% to less than 20%. Taking into account the very low amount of coke deposited on this catalyst after the long reaction time (only 0.46 wt%), the deactivation seems to be mainly due to a sintering process. This fact is supported by TEM and CH dehydrogenation results obtained on fresh and used Pt/Al_2O_3 catalyst. The H_2/CO molar ratio obtained for the Pt(0.5%)/Al_2O_3 catalyst decreases sharply with the reaction time and this effect could be attributed to a higher contribution of the RWGS reaction (which produces CO and consumes H_2), which is favoured on large metallic particles present in the used Pt/Al_2O_3 catalyst [24].

The monometallic Ni(10%)/Al_2O_3 catalyst shows a high activity and a very good stability during the long reaction experiment. The filamentous structure of the carbon formed on this catalyst justifies its stability because the metal particles are on the top of the filaments and thus they continue to be accessible despite the deposition of large amounts of carbon [25]. The addition of a low amount of Pt (0.5 wt%) leads to a better catalytic performance and thus the Pt(0.5%)Ni(10%)/Al_2O_3 catalyst shows higher activity, stability and H_2/CO molar ratio. Although the activity of both samples remained constant along the 6500 min reaction time, both the total carbon deposition and the surface coke, detected by TPO, XPS and TEM, was markedly lower in the bimetallic PtNi catalyst than in the monometallic Ni. Hence, it is expected that the bimetallic catalyst will be more stable at longer reaction times.

Results of the test reaction and chemisorption measurements indicate that geometric effects, such as dilution and blocking, are very important in the bimetallic PtNi catalyst. TPR results show that the reduction of the nickel oxide particles in this sample takes place at much lower temperature than in the monometallic Ni catalyst, which could be due to the close contact between nickel and platinum during the simultaneous reduction of the two oxide precursors. In agreement with the mentioned easier reduction of NiO species, XPS results show that in the bimetallic PtNi catalyst (reduced and used ones) the proportion of Ni^0 is higher than in the monometallic Ni catalyst.

The higher activity and lower carbon deposit of the bimetallic PtNi catalyst (respect to the monometallic Ni) can be related with the presence in this sample of smaller Ni metal particles due to a "dilution" effect of Pt. The homogeneous surface distribution of nickel particles in the close vicinity of Pt leads to a higher activity and favours the formation of more reactive intermediate carbonaceous species, thus maintaining the metallic surface cleaner.

5. Conclusions

From the results presented and discussed above, the following conclusions can be drawn:

- The pronounced deactivation shown by the monometallic Pt(0.5%)/Al_2O_3 catalyst during the 6500 min reaction time of DRM is mainly due to a significant sintering of the metallic phase.
- The monometallic Ni(10%)/Al_2O_3 catalyst shows a high and stable activity along the 6500 min reaction time (both CH_4 and CO_2 conversions keep high and constant values).
- A high and constant activity along the 6500 min reaction time is also featured by the bimetallic Pt(0.5%)Ni(10%)/Al_2O_3 catalyst but the carbon deposition is markedly lower than for the Ni(10%)/Al_2O_3 catalyst.
- The H_2/CO molar ratio is lower than one for the three samples investigated and, associated with the catalysts deactivation, the H_2/CO molar ratio for Pt(0.5%)/Al_2O_3 catalyst decreases from 0.7 to 0.4, while it remains constant and close to 0.6 for Ni(10%)/Al_2O_3 and Pt(0.5%)Ni(10%)/Al_2O_3 ones.
- The addition of platinum (0.5%) to Ni(10%)/Al_2O_3 catalyst decreases the amount of carbon deposited after reaction and this fact tentatively increases the catalyst stability at longer (more than 6500 min) reaction times.

- CH dehydrogenation and chemisorption results indicate that geometric effects (dilution and blocking) would be responsible for the excellent catalytic behaviour of the bimetallic Pt(0.5%)Ni(10%)/Al_2O_3 catalyst.
- TPR and XPS results reveal that the presence of platinum makes the reduction of NiO species easier in the bimetallic catalyst because nickel and platinum are in close contact during the simultaneous reduction of the two oxide precursors. This fact occurs both during reduction step previous to the reaction, and also during the additional reduction that takes place during the long-term reforming reaction.

Acknowledgements

The authors thank Generalitat Valenciana and FEDER (PROMETEO/2009/047) (Spain) and Universidad Nacional del Litoral (Argentina) for financial support. Authors thank M.A. Torres for experimental assistance.

References

[1] J.R. Rostrup-Nielsen, Catal. Today 18 (1993) 305–324.
[2] M.C.J. Bradford, M.A. Vannice, Catal. Rev. Sci. Eng. 41 (1999) 1.
[3] B. Pawelec, S. Damyanova, K. Arishtirova, J.L. Fierro, L. Petrov, Appl. Catal. A: Gen. 323 (2007) 188–201.
[4] C.E. Daza, J. Gallego, J.A. Moreno, F. Mondragón, S. Moreno, R. Molina, Catal. Today 133–135 (2008) 357–366.
[5] K.Y. Koo, H.-S. Roh, Y.T. Seo, D.J. Seo, W.L. Yoon, S.B. Park, Appl. Catal. A: Gen. 340 (2008) 183–190.
[6] E. Ruckenstein, Y.H. Hu, Appl. Catal. A: Gen. 133 (1995) 149–161.
[7] J.G. Seo, M.H. Youn, I. Nam, S. Hwang, J.S. Chung, I.K. Song, Catal. Lett. 130 (2009) 410–416.
[8] A.N.J. van Keulen, M. Hegarty, J.R.H. Ross, P.F. van der Ooesterhamp, Stud. Surf. Sci. Catal. 107 (1997) 537–546.
[9] N. Sahli, C. Petit, A.C. Roger, A. Kiennemann, S. Libs, M.M. Vetar, Catal. Today 113 (2006) 187–193.
[10] J. Wei, E. Iglesia, J. Catal. 224 (2004) 370–383.
[11] J. Juan-Juan, M.C. Román-Martínez, M.J. Illán-Gómez, Appl. Catal. A: Gen. 301 (2006) 9–15.
[12] Y.-G. Chen, K. Tomishige, K. Yokoyama, K. Fujimoto, Appl. Catal. A: Gen. 165 (1997) 335–347.
[13] C. Raab, J.A. Lercher, J.G. Goodwin, J.Z. Shyu, J. Catal. 122 (1990) 406–414.
[14] K. Tomishige, S. Kanazawa, M. Sato, K. Ikushima, K. Kunimori, Catal. Lett. 84 (2002) 69–74.
[15] M. Ocsachoque, F. Pompeo, G. González, Catal. Today 172 (2011) 226–231.
[16] J.C.S. Wu, H.-C. Chou, Chem. Eng. J. 148 (2009) 539–545.
[17] B. Steinhauer, M.R. Kasireddy, J. Radnik, A. Martin, Appl. Catal. A: Gen. 366 (2009) 333–341.
[18] A.D. Cinneide, J.K.A. Clarke, Catal. Rev. 7 (1972) 233.
[19] G. Lietz, H. Lieske, H. Spindler, W. Hanke, J. Völter, J. Catal. 81 (1983) 17–25.
[20] Z. Hou, O. Yokota, T. Tanaka, T. Yashima, Appl. Catal. A: Gen. 253 (2003) 381–387.
[21] C.D. Wagner, L.E. Davis, M.V. Zeller, J.A. Taylor, R.H. Raymond, L.H. Gale, Surf. Interface Anal. 3 (1981) 211–225.
[22] M. García-Diéguez, I.S. Pieta, M.C. Herrera, M.A. Larrubia, L.J. Alemany, Appl. Catal. A: Gen. 377 (2010) 191–199.
[23] T.L. Barr, S. Seal, J. Vac. Sci. Technol. A 13 (3) (1995) 1239–1247.
[24] J. Agrell, G. Germani, S.G. Järås, M. Boutonnet, Appl. Catal. A: Gen. 242 (2003) 233–245.
[25] F. Pompeo, N. Nichio, O. Ferretti, D. Resasco, Int. J. Hydrogen Energy 30 (2005) 1399–1405.